NASA/TM-2005-213785

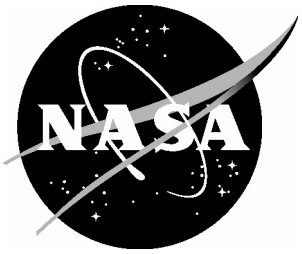

Simulation of Impact on a Ductile Polymer Plate

Rebecca L. Cremona
Brown University, Providence, Rhode Island

Jeffrey A. Hinkley
Langley Research Center, Hampton, Virginia

July 2005

The NASA STI Program Office . . . in Profile

Since its founding, NASA has been dedicated to the advancement of aeronautics and space science. The NASA Scientific and Technical Information (STI) Program Office plays a key part in helping NASA maintain this important role.

The NASA STI Program Office is operated by Langley Research Center, the lead center for NASA's scientific and technical information. The NASA STI Program Office provides access to the NASA STI Database, the largest collection of aeronautical and space science STI in the world. The Program Office is also NASA's institutional mechanism for disseminating the results of its research and development activities. These results are published by NASA in the NASA STI Report Series, which includes the following report types:

- TECHNICAL PUBLICATION. Reports of completed research or a major significant phase of research that present the results of NASA programs and include extensive data or theoretical analysis. Includes compilations of significant scientific and technical data and information deemed to be of continuing reference value. NASA counterpart of peer-reviewed formal professional papers, but having less stringent limitations on manuscript length and extent of graphic presentations.

- TECHNICAL MEMORANDUM. Scientific and technical findings that are preliminary or of specialized interest, e.g., quick release reports, working papers, and bibliographies that contain minimal annotation. Does not contain extensive analysis.

- CONTRACTOR REPORT. Scientific and technical findings by NASA-sponsored contractors and grantees.

- CONFERENCE PUBLICATION. Collected papers from scientific and technical conferences, symposia, seminars, or other meetings sponsored or co-sponsored by NASA.

- SPECIAL PUBLICATION. Scientific, technical, or historical information from NASA programs, projects, and missions, often concerned with subjects having substantial public interest.

- TECHNICAL TRANSLATION. English-language translations of foreign scientific and technical material pertinent to NASA's mission.

Specialized services that complement the STI Program Office's diverse offerings include creating custom thesauri, building customized databases, organizing and publishing research results ... even providing videos.

For more information about the NASA STI Program Office, see the following:

- Access the NASA STI Program Home Page at ***http://www.sti.nasa.gov***

- E-mail your question via the Internet to help@sti.nasa.gov

- Fax your question to the NASA STI Help Desk at (301) 621-0134

- Phone the NASA STI Help Desk at (301) 621-0390

- Write to:
  NASA STI Help Desk
  NASA Center for AeroSpace Information
  7121 Standard Drive
  Hanover, MD 21076-1320

NASA/TM-2005-213785

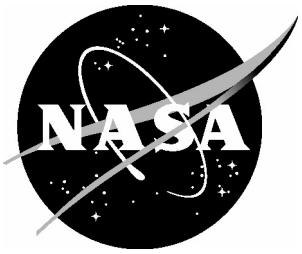

Simulation of Impact on a Ductile Polymer Plate

Rebecca L. Cremona
Brown University, Providence, Rhode Island

Jeffrey A. Hinkley
Langley Research Center, Hampton, Virginia

National Aeronautics and
Space Administration

Langley Research Center
Hampton, Virginia 23681-2199

July 2005

Available from:

NASA Center for AeroSpace Information (CASI)
7121 Standard Drive
Hanover, MD 21076-1320
(301) 621-0390

National Technical Information Service (NTIS)
5285 Port Royal Road
Springfield, VA 22161-2171
(703) 605-6000

Simulation of Impact on A Ductile Polymer Plate

Rebecca Cremona, Brown University
Jeffrey A. Hinkley, NASA Langley Research Center

Abstract

Explicit finite element calculations were used to visualize the deformation and temperature rise in an elastic-plastic plate impacted by a rigid projectile. Results were compared to results of experiments involving ballistic penetration of a "self-healing" thermoplastic. The calculated temperature rise agreed well with the experimental observation, but the total energy absorbed in the penetration event was underestimated in the calculation, which neglected friction.

Introduction

When plants and animals sustain damage, they can often heal and regain some of their lost function. Inspired by this capability of living systems, technologists have sought to design "self-healing" synthetic materials. Several lines of research are being pursued: composites that contain crack-filling reagents, self-assembled layers of various sorts, and -- the subject of this report -- thermoplastics that flow to seal a ballistic puncture (1,2). The initial work employed Surlyn® 8920 (a duPont™ product). Since then, several other such self-healing thermoplastics have been identified (3), but the healing mechanism is not fully understood. Because the healing occurs in much less than one second, few experimental techniques are applicable. The present report, therefore, applies finite element (FE) analysis in an effort to identify important features of the impact event.

Methods

TOCHNOG, a free open-source software package (4), was used. Although not as versatile as some commercial packages, it has a number of useful features including contact (implemented with a penalty formulation), new mesh generation to correct distorted elements, and the ability to handle thermal convection and diffusion as well as material velocities and stresses. In TOCHNOG, velocities, rather than displacements, are the primary variables and variables (assumed to be continuous) are stored in element nodes. An explicit integration scheme was chosen. A sample TOCHNOG script is given in the Appendix.

The polymer constitutive law was elastic-perfectly plastic with a von Mises yield criterion. Previous work (5) has shown that this is a good starting point for this type of simulation. Initial properties were chosen to be similar to those of Surlyn® at room temperature (Table 1). Models were 2-dimensional with axisymmetry. Friction was neglected. Nodes at the circumference of the target were fixed to simulate a clamped boundary and the horizontal velocity was constrained to zero along the centerline. For most of the calculations, the plate radius was 15mm, i.e. about 3

The use of trade names of manufacturers does not constitute an official endorsement of such products or manufacturers, either expressed or implied, by the National Aeronautics and Space Administration.

times the radius of the rigid projectile. The initial conditions corresponded to the undeformed state (zero strain and temperature).

Table 1. Initial Assumed Properties of Target material

Young's Modulus, E, MPa	*350*
Poisson's Ratio, ν	*0.4*
Tensile yield stress, σ_{ys}, MPa	*15*
Density, kg/m^2	*950*
Tensile failure strain, %	*470*

Finite element results were visualized with the postprocessor in GiD (6).

Results and Discussion

In the experimental ballistic tests described in Reference 1, the only data available are a) the change in bullet velocity, b) full-field infrared thermographic temperatures obtained a few tenths of a second after penetration, and c) the appearance of the specimen post-impact. Taken together, this is not enough information to quantitatively validate a finite element model. Nevertheless, it is of interest to study the effects of the model assumptions in a parametric way.

Dynamics of Impact: As a first demonstration of the software's capability, consider a model of a 50 mm-radius x 6 mm-thick plate impacted by a rigid sphere moving downward at a constant speed of 2.6 m/sec. After 3.5×10^{-3} sec, (Figure 1), there is a localized dent, as well as significant global bending and stretching of the plate. Due to the axisymmetry, only half the plate is shown. When the projectile velocity is 260 m/sec (characteristic of a pistol bullet), on the other hand, Figure 2 illustrates the result. At the ballistic rate, the polymer deformation is highly localized and the global plate response appears to be negligible. The amount of projectile travel in Figure 2 is the same as in Figure 1 although the scale of the visualization is slightly different.

Deformation and Failure: A complete description of the plate penetration would require *i*) a realistic constitutive model and *ii*) a failure criterion. To simulate healing, the material description would have to include in addition *iii*) nonlinear viscoelastic recovery, *iv*) melting, *v*) surface tension, and *vi*) interdiffusion. While finite element methods are able in principle to handle these effects, only the initial deformation is treated in this report.

Investigators of the self-healing thermoplastics have considered various different projectiles: Fall (1) used conventional pistol bullets, which have an elliptical ogive with a length/diameter ratio close to unity. This rounded profile meets the symmetry axis with zero slope, so it is similar to the spherical profile modeled here (Figure 3). The pellets used by Kalista et al. (2) had somewhat blunted conical points, whereas the point of rifle bullets is often a spitzer ogive, which is a surface of revolution of a circular arc that is tangent to the shank. Figure 4 is an example of this kind of point, although in this case, the cylindrical shank of the bullet was not modeled. Finally, Fall showed that flat-ended cylinders left a hole that did not heal completely. A simulation of this case is shown in Figure 5. The response in the vicinity of the sharp corner of

this projectile is not captured correctly; attempts to use a finer mesh seemed to lead to numerical problems and the calculation could not be completed.

As mentioned in the preceding section, the plate deformation in Figures 3-5 is confined to a fairly small region (not much beyond the projectile radius). The region of the very highest strains is a thin layer (less than 1 mm) immediately adjacent to the projectile. Figure 3 gives a good indication of the role of ductility in the penetration process. Even though the "bullet" has traveled a distance equal to nearly twice the initial thickness of the plate, the maximum principal strain (which occurs under the sphere) is still less than the tensile failure strain of Surlyn. In Figure 5 on the other hand, the thinnest region of the plate is adjacent to the corner of the cylinder. It is easy to imagine that continued thinning would lead to detachment of a plug of material. This failure mode would explain the lack of healing in this case (which is what Fall hypothesized was occurring with blunt cylindrical projectiles).

Most published ballistics work involves metals and concrete. Perforation mechanisms have been reviewed (7) and include fragmentation, spalling, petalling, and plugging. A few studies on penetration of polymethylmethacrylate (8,9) and polycarbonate (10) indicate that the failure geometry depends on projectile shape, panel thickness, and strain rate. After being struck by a pistol bullet, some healed Surlyn plates contain fine radial lines that suggest that petalling may have occurred. This failure mode cannot, of course, be captured by a 2D simulation, and should be a subject for future work. In addition, a more sophisticated description of the post-yield mechanical behavior will probably be needed eventually: the constitutive model used in the present report includes neither strain-hardening nor damage accumulation. A final complication not treated here arises from the likelihood that the texture of *semicrystalline* polymers may evolve differently under multiaxial (as opposed to uniaxial) stretching. This means that material properties obtained in simple tension may not be relevant to the puncture experiment (11).

Energy Absorption: Many approximate treatments of terminal ballistics have been proposed. Most closed-form expressions are either semiempirical energy-balance fits or they are based on the solution for the stress at the surface of an expanding spherical cavity (12). To employ the latter, the radial cavity stress is decomposed into tangential and axial components. Integrating the axial stress over the nose of a hemispherical projectile gives the assumed force on the nose:

$$F = \pi a^2\{A+\rho_t[(2/3)a(dV/dt) + 3V^2/4]\} \qquad (1)$$

Where a is the hemisphere radius, V is the rigid-body projectile velocity, t is time, and ρ_t is the target density (14). The elastic-plastic material constant $A = (2\sigma_{ys}/3)[1 + \ln (2E/3\sigma_{ys}]$. Neglecting friction and using the properties in Table 1 and an initial velocity of 260 m/sec, one calculates a deceleration of $2.9x10^3$ m/sec/m. For a plate whose thickness is comparable to the bullet diameter (as in the experiments in references 1 and 2), the average deceleration would be expected to be lower, for the following reasons. In the early stages of penetration, the contact area would be less than the full hemisphere that was used in the closed-form solution, and in the later stages, the plastic region would not be constrained by elastic material (which is the implicit assumption of the spherical cavity solution).

Next, deceleration of a bullet was simulated using finite elements. A spherical projectile was given an initial velocity and mass that match those of the copper-jacketed 9 mm slugs used in experiments at LaRC (13). Figure 6 shows simulated projectile velocity as a function of distance for three different panel thicknesses calculated using the polymer properties in Table 1. For the thickest panel, the initial slope corresponds to about 1.1×10^3 m/sec velocity change per meter of travel. This is lower than the closed form result, as expected, and has the right order of magnitude. The sensitivity of this FE result to the material properties was explored using the variations in Table 3. These results are shown in Figure 7.

Table 3. Constitutive parameters for sensitivity study in Figure 7.

	Modulus, MPa	Yield Stress, MPa
Case I	350	15
Case II	700	15
Case III	350	30
Case IV	700	30

The curves in Figures 6 and 7 are fairly featureless, except for a decrease in slope as the projectile nears the back surface of the plate and the polymer thins out. The sensitivity study shows that increases in either the polymer's modulus or its yield stress would lead to more rapid deceleration of the projectile. These material properties will be revisited in the next section.

The elastic-plastic model used here does not include a failure criterion, so it is not possible to predict the total expected velocity change with any accuracy. Upon examining Figure 3, however, it seems unlikely that a 6-mm panel would provide much additional resistance beyond, say, 12 mm of projectile travel. This would imply, from the FE results, a final velocity on the order of 250 m/sec.

Experimentally, the velocity changes are much larger (Table 2). It therefore seems that factors omitted from the simulation -- friction, viscoelastic dissipation, elastic dishing of the plate, and possibly boundary effects -- play large roles in slowing the projectile.

Table 2 Slowing of 9-mm Pistol Bullets by Surlyn (Ref. 13) (averages of 2 trials)

Panel thickness, mm	Initial velocity, m/sec	Final velocity, m/sec
6.477	249	203
4.55	263	225
2.26	258	239

Rate and Temperature Effects: The time- and temperature-varying behavior of amorphous polymers near Tg has received a great deal of study. Consider first the time (rate) dependence.

The model proposed by Matsuoka (15) suggests that glassy modulus should scale with a power of the strain rate. The exponent should be about m/2, where $m \approx 1/3$ is the power law exponent of a creep curve. Although Surlyn is not glassy at room temperature, the creep compliance data of Fall (1) are consistent with $m \approx 0.39$. The nominal strain rate of the ballistic penetration is about $30x10^3\ sec^{-1}$, whereas the ASTM D638 tensile test (source of the data in Table 1) occurs at $\sim 1\ sec^{-1}$. The effective modulus at ballistic rates could therefore be $(30x10^3)^{1/6}=5.6$ times higher. Low-rate puncture tests conducted on Surlyn at various rates (3) imply that the yield stress σ_{ys} is also likely to be at least twofold higher at the higher rate. For comparison, a similar factor of 2 would be inferred from rate-dependent tensile yield data on polycarbonate (16).

When plastic work is done on a material, a fraction of that work (often symbolized by β) is converted to heat. For metals $\beta \approx 0.9$, but for polymers it tends to be lower (17) and $\beta \approx 0.5$ is an appropriate rule-of-thumb. The storage of "plastic" (actually anelastic) strain energy is the reason that polymer strains of at least 60% can be nearly completely recoverable (18). Representative values were chosen for polymer thermal conductivity (0.172 W/mK) and heat capacity (1.6 kJ/kgK). Incorporating heat generation with $\beta = 0.5$ in the FE calculations, it was found that temperatures climbed more than 50°C above ambient in a narrow zone near the projectile (Figure 8). This prediction matches reasonably well with the temperature rise seen experimentally (1).

The properties of polymers are strongly dependent on temperature, so this temperature rise should, in turn, affect the mechanical properties. For this parametric study, the high-rate modulus and yield stress derived above were both allowed to decline linearly with temperature, reaching zero at the polymer melting point (~90°C). Figure 9 shows the calculated effect of thermomechanical coupling on energy absorption.

Conclusions

It was shown that polymer deformation under projectile impact is highly localized and should produce very localized heating. With a rounded projectile, strains are highest below the nose of the bullet and a highly ductile polymer may exhibit different failure modes than metals do. Directions for future work have been identified.

References

1. R. Fall, "Puncture Reversal of Ethylene Ionomers-Mechanistic Studies". MS Thesis, Virginia Tech, 2001. http://scholar.lib.vt.edu/theses/available/etd-08312001-084412/
2. S. J. Kalista, Jr., T. C. Ward, and Z. Oyetunji, Proceedings of the 26th Annual Meeting of The Adhesion Society, 2003, pp 176-178. Also Kalista, S.J. Jr., MS Thesis, Virginia Polytechnic Institute, http://scholar.lib.vt.edu/theses/available/etd-12162003-103411/
3. A. Huber and J. A. Hinkley, "Impression Testing of Self-Healing Polymers," NASA/TM-2005-213532, March 2005, http://hdl.handle.net/2002/15098.
4. TOCHNOG, by Dennis Roddeman, http://tochnog.sourceforge.net/
5. D. G. Fesco, "Post-Yield Behavior of Thermoplastics and the Application to Finite Element Analysis" Polym. Eng. Sci. 40, 1190 (2000).
6. GiD, International Center for Numerical Methods in Engineering, CIMNE, http://www.gid-usa.com/index.html
7. G. C. Corbett, S. R. Reid, and W. Johnson. "Impact loading of Plates and Shells by Free-Flying Projectiles: A Review" Int'l. J. Impact Eng. 18(2), 141 (1996).
8. S. Ogihara, T. Ishigure, A. Kobayashi. "Study on Impact Perforation Fracture Mechanism in PMMA" J. Mater. Sci. Lett. 17(8), 691 (1998).
9. M. Segreti, A. Rusinek, and J. R. Klepaczko. "Experimental Study on puncture of PMMA at low and high velocities, effect on the failure mode" Polymer Testing 23, 702 (2004).
10. S. C. Wright, N. A. Fleck, and W. J. Stronge "Ballistic Impact of Polycarbonate-An Experimental Investigation". Intl. J. Impact Eng. 13(1), 1(1993).
11. O. Shang, N. Billon, J. M. Muracciole, and F. Fernagut, "Mechanical Behavior of a Ductile Polyamide 12 During Impact" Polym. Eng. Sci. 36, 541 (1996).
12. See the review in X. W. Chen and Q. M. Li, "Perforation of a thick plate by rigid projectiles" Int. J. Impact. Engng. 28, 743 (2003).
13. R. Cano (Langley Research Center), personal communication.
14. M. J. Forrestal, D. Y. Tzou, E. Askari, and D. B. Longcope, "Penetration into ductile metal targets with rigid spherical-nose rods", Int. J. Impact Engng. 16, 699 (1995).
15. S. Matsuoka, "Relaxation Phenomena in Polymers", Hanser, Munich, 1992 Chapter 3.
16. J. Richeton, S. Ahzi, L. Daridon, and Y. Remond. "Modeling of strain rates and temperature effects on the yield behavior of amorphous polymers" J Phys IV, France 110. 39 (2003).
17. O. B. Salamatina, S. N. Rudnow, V. V. Voenniy, and E. F. Oleynick "Heat and Stored Energy of Plastic Deformation of Solid Polymers and Heterogeneous Blends" J. Thermal Anal. 38, 1271 (1992).
18. T. Ricco and A. Pegoretti "Energy Storage and Strain-Recovery Processes in Highly-deformed Semicrystalline Poly(butylene-terephthalate)", J. Polym. Sci. (Phys) 40, 236 (2001).
19. Z. Li and J. Lambros "Strain Rate Effects on the Thermomechanical Behavior of Polymers" Intl. J. Solids and Structures 38, 3549 (2001)

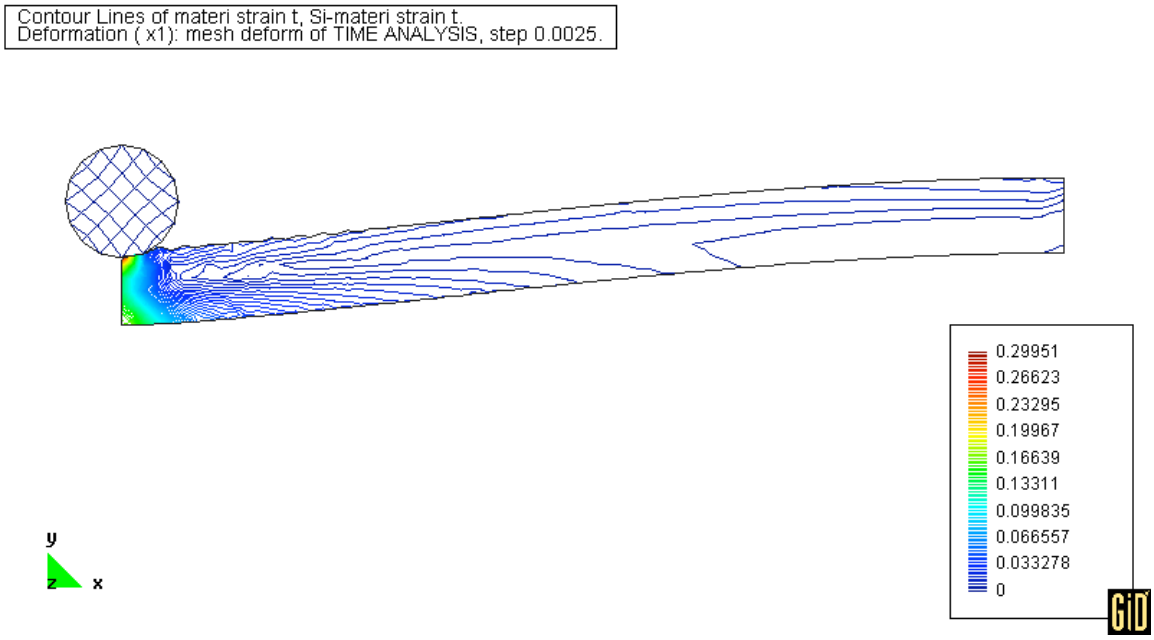

Figure 1. Low-rate impact (2.6 m/sec) on polymer plate. Sphere is moving downward.

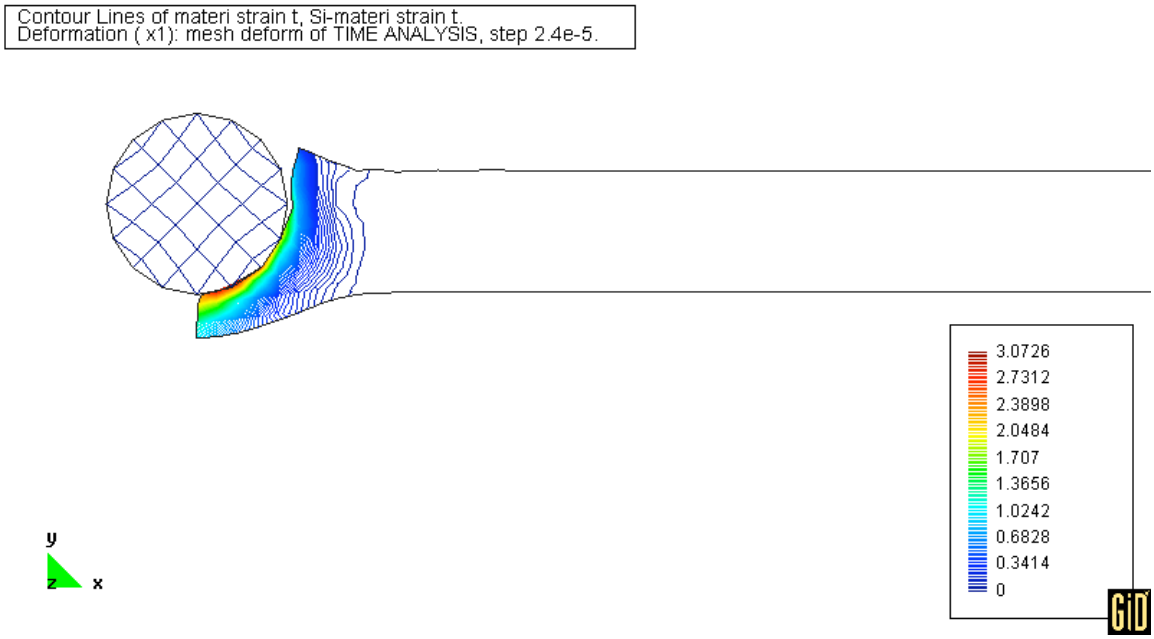

Figure 2. High-rate impact (260 m/sec) on polymer plate.

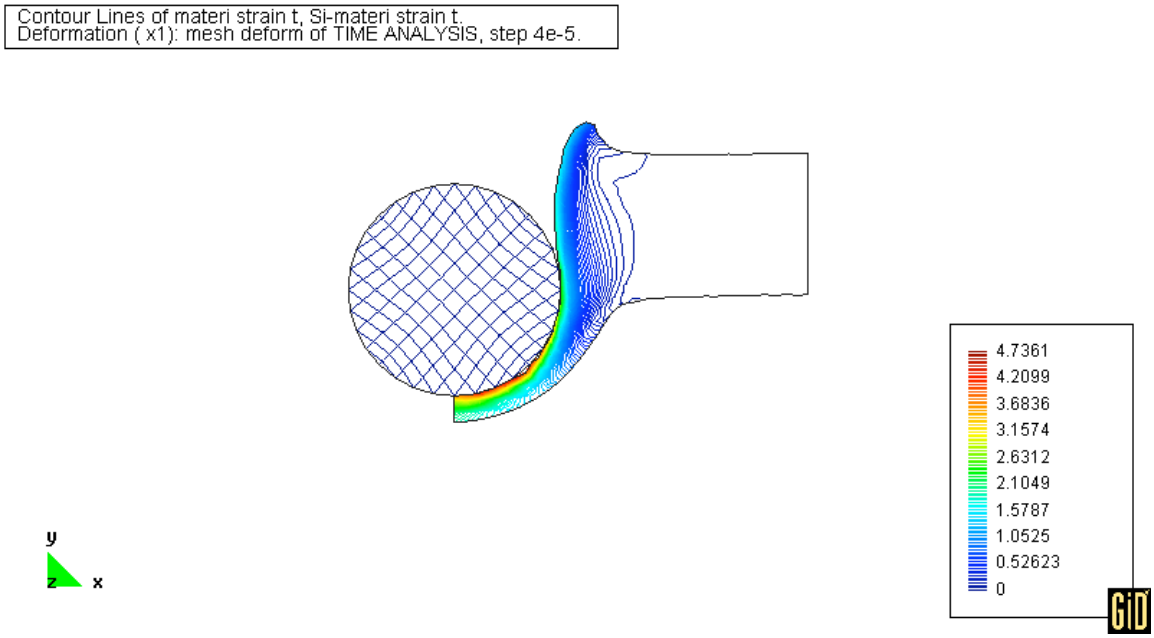

Figure 3. Deformation by impact of sphere on elastic-plastic plate.

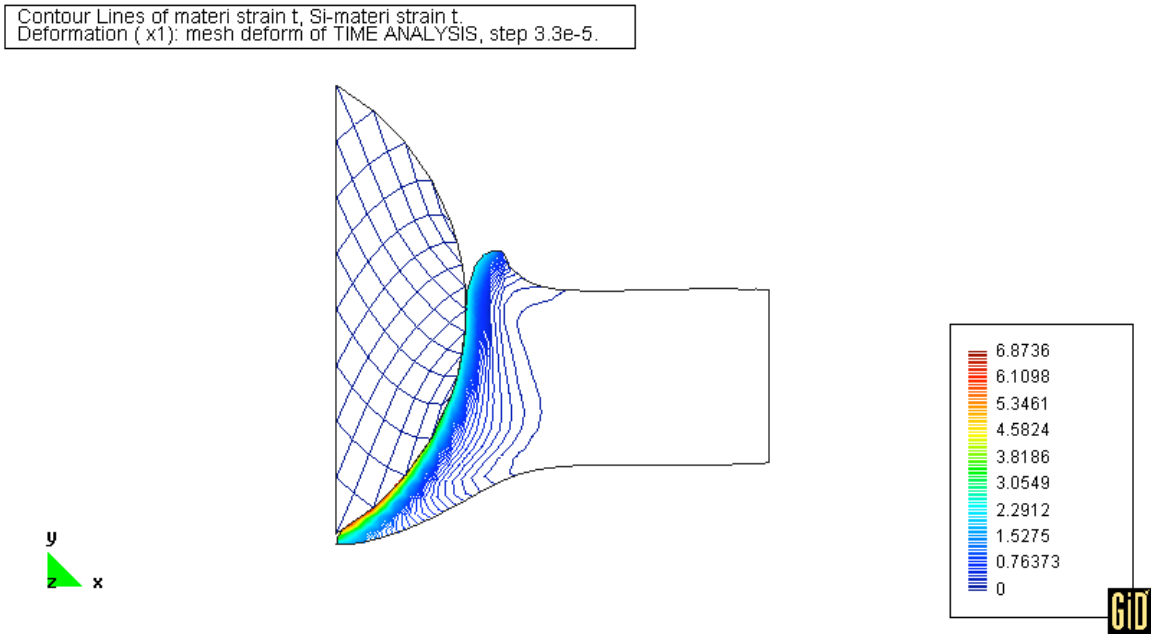

Figure 4. As Figure 3, with ogival projectile.

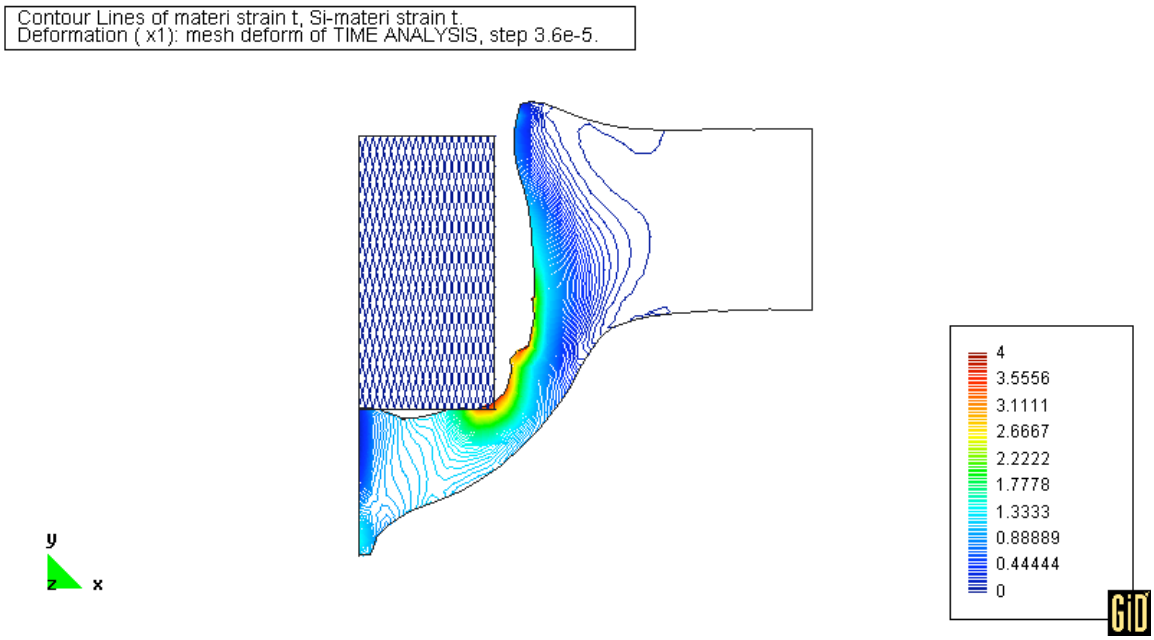

Figure 5. As in Figures 3 and 4, but with cylindrical projectile.

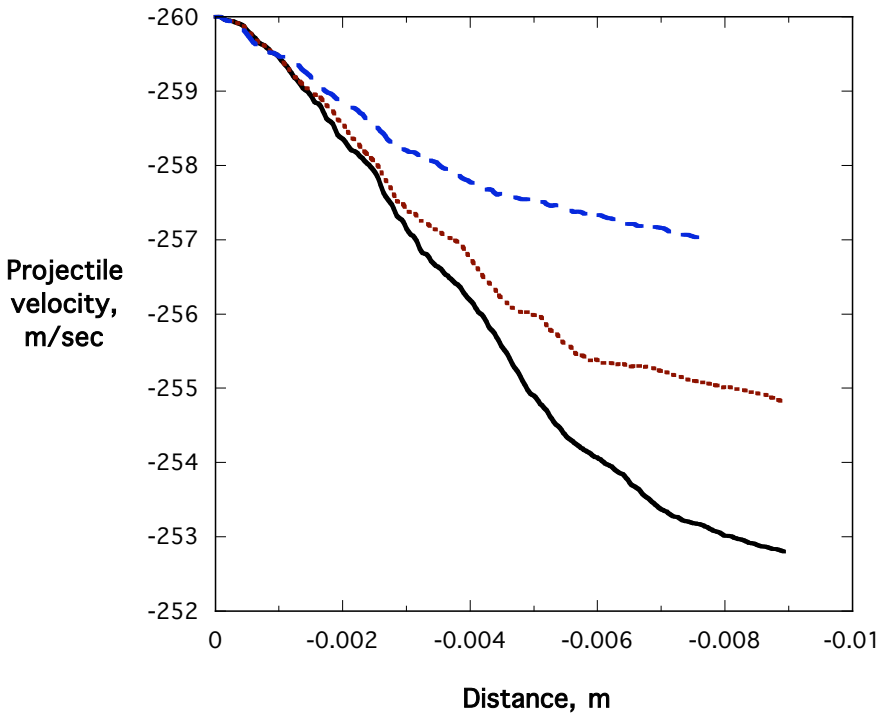

Figure 6. Calculated velocity of spherical projectile vs. distance for three plate thicknesses. Solid line: 6 mm plate; dotted line, 4 mm; dashed line, 2 mm.

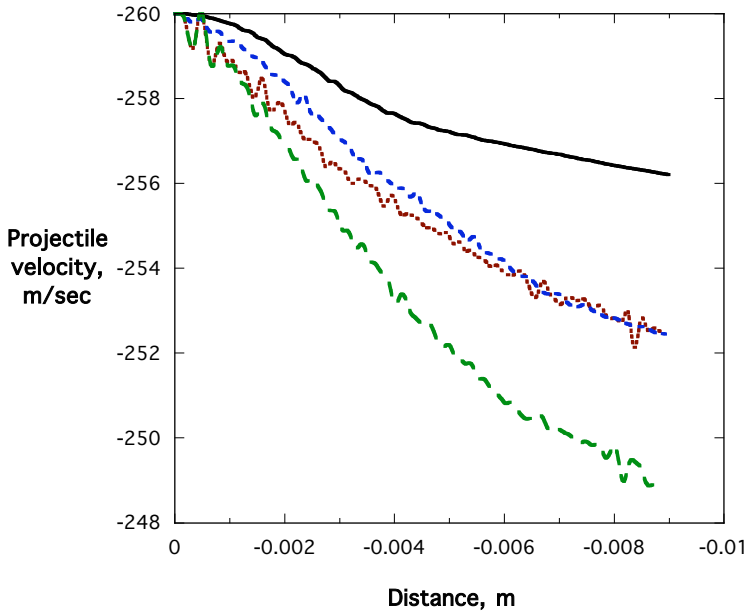

Figure 7. Effect of polymer properties listed in Table 3 on deceleration of a spherical projectile impacting a 6-mm-thick plate. Solid: Case I; dotted, case II; short dashes, case III; long dashes, case

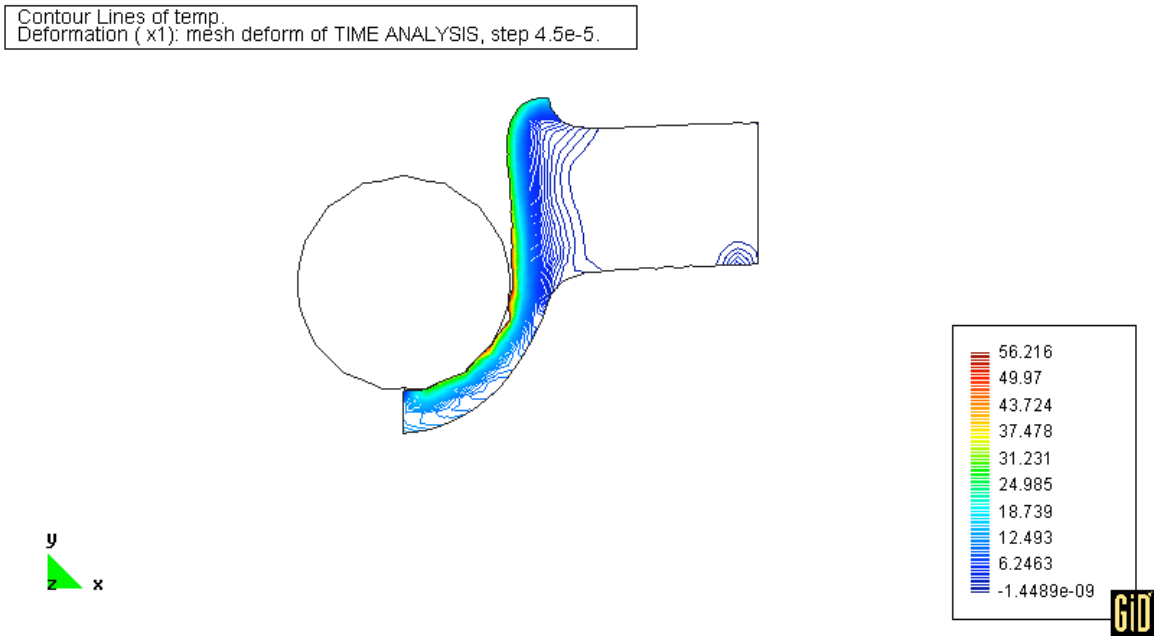

IV

Figure 8. Temperature contours (°K above ambient) for impact. Temperature-independent material properties.

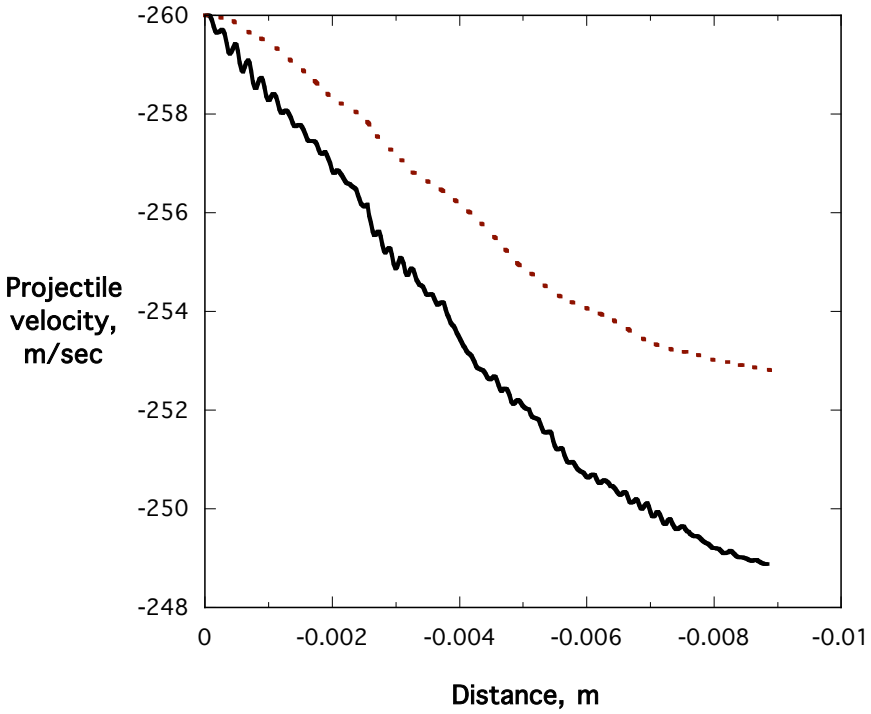

Figure 9. Effect of thermomechanical coupling. Solid line: constant modulus and yield strength; dotted line: with softening due to plasticity-induced heating as described in the text.

Appendix

A listing of a TOCHNOG script follows. Comments in parentheses are ignored by the program.

```
(axisphere10)

(initiation section)
(echo script to screen)
echo -yes
number_of_space_dimensions 2
(declare variables to store in each node)
(condif=conduction and diffusion of heat)
condif_temperature
materi_velocity
materi_stress
(plastic strain)
materi_strain_plasti
materi_strain_total
(kappa=effective accumulated scalar plastic strain)
materi_plasti_kappa

end_initia

(bullet)
(point centered on circle with 4.51mm tolerance)
geometry_point 1 0 4.5e-3 4.51e-3
(mesh a circle and refine mesh twice)
control_mesh_macro 1 -circle 0 2
(set boundary nodes for detecting contact)
control_mesh_macro_set_node_boundary 1 –yes
(locate circle at [0,4.5mm] with 4.5 mm radius)
control_mesh_macro_parameters 1 0 4.5e-3 4.5e-3
(location to follow bullet movement during postprocessing)
post_point 1 0 4.5e-3

(bullet material properties: stiff, elastic)
group_type 0 -materi
group_materi_elasti_young 0  1e13
group_materi_density 0 19.58e3
group_materi_elasti_poisson  0 0.3
group_axisymmetric 0 -yes

(constrain x-coordinates of bullet nodes (zero velocity))
bounda_unknown 13 -geometry_point 1  -velx
bounda_time 13 0
(apply initial velocity in y-direction)
(select nodes to apply to)
```

```
control_data_put      15  -node_dof -geometry_point 1
(assign initial values to all variables)
control_data_put_double  15   0. (temp)
                              0. -260    (Vx and Vy )
                              0. 0. 0. 0. 0. 0.  ( stress )
                              0. 0. 0. 0. 0. 0.  ( plas strain )
                              0. 0. 0. 0. 0. 0.  ( totl strain)
                              0. ( kappa )

(plate)
group_type 1 -materi -condif
group_condif_density 1 950
group_condif_conductivity 1 0.172
group_condif_capacity 1  1.6e3
group_materi_elasti_young 1  1960e6
group_materi_plasti_vonmises 1 30e6
group_materi_density 1 950
group_materi_elasti_poisson  1 0.4
group_materi_plasti_heatgeneration 1 0.5
group_materi_memory 1 –updated
(Young's modulus and yield stress dependence on temperature)
dependency_item 4 -group_materi_elasti_young 1 -temp 3
(piecewise linear: from temp=0 (ambient) to 70; 70 to 200)
dependency_diagram 4 0 70 200 1960e6 0 0
dependency_item 6 -group_materi_plasti_vonmises  1 -temp 3
dependency_diagram 6 0 70 200 30e6 0 0

group_axisymmetric 1 -yes

control_mesh_macro 20 -rectangle 1 10 4
(plate is 15mmx6mm)
control_mesh_macro_parameters 20  7.5e-3 -3.1e-3 15e-3 6e-3
control_mesh_macro_element  20  -quad4
control_mesh_macro_set_node_boundary 20 -yes
(clamped edge)
geometry_line 3 15e-3 -10e-3 15e-3 10e-3 0.1e-3
(center line)
geometry_line 4 0 -7e-3 0 -0.1e-3 0.1e-3
(boundary conditions)
bounda_unknown   5 -geometry_line 3 -vely -velx
bounda_time      5 0.0 0.0 100.00  0.0
bounda_unknown   7 -geometry_line 4 -velx
bounda_time      7 0.0 0.0 100.00  0.0

contact_penalty_velocity 1e7
(turn off "stabilization" (useful for quasistatic case only))
options_stabilization  -no
```

```
(generate completely new mesh for plate; 0.5 mm elements)
control_mesh_new_mesh 30 .0005
control_mesh_new_mesh_element 30  -quad4
control_mesh_new_mesh_region 30 1

(take 50 steps of 0.1 microsecond)
control_timestep  40  1e-7  50e-7
(explicit calculation)
control_timestep_iterations 40 1
(print time and projectile speed to screen for each step)
print_filter 1 -post_point_dof 1 -vely
control_print  40  -time_current -post_point_dof
(save data to file)
control_print_data_versus_data 40  -time_current 0 0 -
post_point_dof 1 2

(save output files for visualization)
control_print_gid 45 -separate
(loop back to statement 30 and repeat 8 more times)
control_repeat 50 8 30

end_data
```

REPORT DOCUMENTATION PAGE

Form Approved
OMB No. 0704-0188

1. REPORT DATE *(DD-MM-YYYY)*	2. REPORT TYPE	3. DATES COVERED *(From - To)*
01- 07 - 2005	Technical Memorandum	

4. TITLE AND SUBTITLE
Simulation of Impact on a Ductile Polymer Plate

5a. CONTRACT NUMBER

5b. GRANT NUMBER

5c. PROGRAM ELEMENT NUMBER

6. AUTHOR(S)
Cremona, Rebecca L; and Hinkley, Jeffrey A.

5d. PROJECT NUMBER

5e. TASK NUMBER

5f. WORK UNIT NUMBER
23-064-50-10

7. PERFORMING ORGANIZATION NAME(S) AND ADDRESS(ES)
NASA Langley Research Center
Hampton, VA 23681-2199

8. PERFORMING ORGANIZATION REPORT NUMBER
L-19149

9. SPONSORING/MONITORING AGENCY NAME(S) AND ADDRESS(ES)
National Aeronautics and Space Administration
Washington, DC 20546-0001

10. SPONSOR/MONITOR'S ACRONYM(S)
NASA

11. SPONSOR/MONITOR'S REPORT NUMBER(S)
NASA/TM-2005-213785

12. DISTRIBUTION/AVAILABILITY STATEMENT
Unclassified - Unlimited
Subject Category 27
Availability: NASA CASI (301) 621-0390

13. SUPPLEMENTARY NOTES
Cremona: Brown University; Hinkley: Langley Research Center
An electronic version can be found at http://ntrs.nasa.gov

14. ABSTRACT

Explicit finite element calculations were used to visualize the deformation and temperature rise in an elastic-plastic plate impacted by a rigid projectile. Results were compared to results of experiments involving ballistic penetration of a "self-healing" thermoplastic. The calculated temperature rise agreed well with the experimental observation, but the total energy absorbed in the penetration event was underestimated in the calculation, which neglected friction.

15. SUBJECT TERMS
Finite element; Self-healing; Polymer; Ballistic; Plasticity

16. SECURITY CLASSIFICATION OF:			17. LIMITATION OF ABSTRACT	18. NUMBER OF PAGES	19a. NAME OF RESPONSIBLE PERSON
a. REPORT	b. ABSTRACT	c. THIS PAGE			STI Help Desk (email: help@sti.nasa.gov)
					19b. TELEPHONE NUMBER *(Include area code)*
U	U	U	UU	19	(301) 621-0390